Publications

Available Online

J. Sci. Res. **4** (3), 541-550 (2012)

JOURNAL OF
SCIENTIFIC RESEARCH
www.banglajol.info/index.php/JSR

The Effect of Cobalt Doping in Structural Phase Transition of $SmFe_{1-x}Co_xAsO$ Measured by Low-temperature X-ray Diffraction

A. Khan[1], A. Rahman[1], S. Naher[1*], H. Kaneko[2], Y. Yun[2], A. Savinkov[2], H. Suzuki[2], Y. K. Li[3], Q. Tao[3], G. H. Cao[3], and Z. A. Xu[3]

[1]Department of Physics, Shahjalal University of Science and Technology, Sylhet-3114, Bangladesh

[2]Department of Physics, Kanazawa University, Kakuma-machi, Kanazawa 920-1192 Japan

[3]Department of Physics, Zhejiang University, Hangzhou 310027, China

Received 1 April 2012, accepted in final revised form 20 June 2012

Abstract

The parent compound SmFeAsO shows structural phase transition from tetragonal to orthorhombic at the temperature T_D = 144 K. In the compound $SmFe_{1-x}Co_xAsO$, with increasing x the structural transition temperature T_D and SDW T_N decreases and reaches 0 K at the critical concentration x_c. The X-ray diffraction technique has been used here to study the structural phase transition temperature. It is observed that the (400) peak of the parent compound SmFeAsO splits into two peaks (400) and (040), when the temperature is lower than the structural transition temperature T_D. The structural phase transition of Co doped compounds $SmFe_{1-x}Co_xAsO$ has also been studied for x = 0, 0.01, 0.025 and 0.075. The phase transition temperature T_D for $SmFe_{0.99}Co_{0.01}AsO$, $SmFe_{0.975}Co_{0.025}AsO$ and $SmFe_{0.925}Co_{0.075}AsO$ are 134 K, 118 K and 4 K, respectively. The phase diagram of T_D versus lattice spacing reveals that the structural transition temperature decreases with shrinking lattice constant along c-axis similar to the decrease of the structural phase transition temperature with increasing Co concentration. The phase diagrams of $SmFe_{1-x}Co_xAsO$ and $Sm(O_{1-}xF_x)FeAs$ show a similar nature.

Keywords: $SmFe_{1-x}Co_xAsO$; Structural phase transition; Co concentration; X-ray diffraction

doi: http://dx.doi.org/10.3329/jsr.v4i3.10248 J. Sci. Res. **4** (3), 541-550 (2012)

1. Introduction

Studies show that since the discovery of cuprate superconductors, relatively high-temperature superconductors in layered pnictide-oxide compounds LnFePnO (Ln = lanthanides, Pn = P, As) has drawn a lot of interest when the new class of compounds ReFeAsO (Re = Sm, Nd, Pr, Ce, La) have been prepared [1]. It is interesting to note that this ReFeAsO is itself a non-superconducting material. The structural phase transition and antiferromagnetic (AFM) ordering associated with Fe ions in all FeAs-based parent

---

[*] *Corresponding author*: shumsun_phy@yahoo.com

compounds lies in the temperature range of 100-200K [2-4]. The low temperature x-ray diffraction study of ReFeAsO (Re = La, Sm, Gd and Tb) shows that the structural phase transition of these parents compound are driven magnetically. In this system both the c-axis and a-axis lattice constant decreases significantly as the radius of the Re changes from the bigger ion radius to the smaller radius and the structural phase transition temperature also decreases monotonously as the ions radius decreases [5].

Various Chemical doping approaches can suppress the structural transition and the AFM order and consequently high T_c superconductor appears. The maximum T_C of fluorine-doped iron-based Layered La[$O_{1-x}F_x$]FeAs (x = 0.05-0.12) family is 26 K [1] and is enhanced up to 43 K under 4 GPa [6]. The unit cell of these compounds contain two molecules, represented by the chemical formula (La_2O_2)(Fe_2As_2). The Fe_2As_2 layer is sandwiched between the La_2O_2 layers. Fe_2As_2 acts as a conducting layer and La_2O_2 as an insulating layer. In replacing O^{2-} with F^- , the parent compound becomes a superconductor. With the help of fluorine-doping the maximum T_C of Sm[$O_{1-x}F_x$]FeAs family (x = 0.20) and Ce[$O_{1-x}F_x$]FeAs become 54 K and 41 K respectively [7-8]. Room temperature XRD studies of these compounds shows that with increasing F^- both a-axis and c-axis decreases monotonically [1, 8-10]. But F^- doping is very difficult particularly in GdFeAsO systems [11-12]. By Thorium (Th^{4+}) substitution for Gd^{3+} in GdFeAsO, the superconductivity is observed to be at 56 K. The Th-doping expands the lattice within the ab-planes but shrinking occurs along c-axis [13]. The superconductivity also occurs in ReFeAsO_{1-x} (Re = Sm, Nd, Pr, Ce, La) by oxygen deficiency in the ReO layer instead of F^--doping [14-15]. However, the theoretical calculations for the electron density by G. Xu et al [16] suggests that substitution of cobalt for iron is expected to induce electrons directly into the FeAs layers. Therefore, it is more interesting to observe the effect of cobalt-doping effect in a ReFeAsO system.

Layered crystal structure of $ReFe_{1-x}Co_xAsO$ is made by sandwiching FeAs layers with ReO layers. The crystal structure of this system is of the ZrCuSiAs type. In these systems carriers are directly doped within the FeAs layer by substitution of Co in the tri-valance Co^{3+} state in the place of Fe^{2+}. With increasing Co concentration, the structural phase transition temperature (T_D) and the AFM ordering temperature (T_N) decrease and reach 0 K at the critical concentration. The maximum value of T_C occurs near the critical concentration x_C, suggesting the QCP which we have already reported [17]. Domelike T_C(x) curves are widely observed in these iron-based pnictides, i.e., Co-doped $LaFe_{1-x}Co_xAsO$ and $SmFe_{1-x}Co_xAsO$ system showing a maximum of T_c 17.2 K [18].

In this paper, we report the investigation of the structural phase transition with increasing Co concentration in $SmFe_{1-x}Co_xAsO$ measured by low-temperature X-ray diffraction. X-ray scattering studies on the ReFeAsO (R=La, Sm, Gd and Tb) samples at room temperature, have shown that, as Re is changed from La through Sm and Gd to Tb, both the c-axis and a-axis lattice constants decrease significantly. This study shows that as the ions radius decreases the lattice constant also decreases. Also the low temperature X-ray diffraction study on these samples show that the structural phase transition temperature also decreases monotonously as the ions radius decreases [5]. The study on the polycrystalline samples of $LFe_{1-x}Co_xAsO$ (L=La and Sm) at room temperature shows that Co doping causes the shrinkage of the c-axis significantly, while the *a*-axis remains nearly unchanged [18-20]. Also shrinkage of the c-axis occurs by the substitution of F^- in $La[O_{1-x}F_x]FeAs$ and $Sm[O_{1-x}F_x]FeAs$ [1, 10]. Similarly, we observed that structural phase transition decreases with decreasing the lattice constant along the c-axis. It is to noted here that if we compare our experimental results with the F^- doped $Sm[O_{1-x}F_x]FeAs$ families, the phase diagram is very similar for the two systems.

2. Samples and Experiments

The polycrystalline sample preparation method was discussed in ref. [18] and we used the same samples. The X-ray diffractometer was RINT 2500 system (Rigaku Co.) with a specially designed goniometer. The X-ray beam was produced under the condition of 45 kV-300mA with rotating Cu anode. Two different types of cooling systems were used to perform our experiment. The specimens were cooled to about 10 K by a cryo-cooler with circulating ^4He gas and also cooled to about 0.1 K using a ^3He-^4He dilution refrigerator. At several temperatures, the entire profiles of the reflection peaks were measured with a step size of 0.001 and a step-counting time 6S. These profiles were refined by the Rietveld method using the reported crystal structure. To get the more precise results, XRD were measured with a step size of 0.005^0 and a step-counting time of 60s for some reflection planes. The profiles at different temperatures are fitted with the Pseudo-Voight function to get the lattice constant d of the (400) peak, the integrated intensity (II) and also the FWHM.

2.1. *SmFeAsO (parent compound x = 0)*

After synthesis the X-ray diffraction at 300K displayed that the crystal has tetragonal structure with *P*4/*nmm* space group having lattice parameters a=0.393726 nm and c=0.849808 nm [18]. Profiles of the Θ-2Θ scans of the (400) reflection of the tetragonal unit cell of SmFeAsO at 200 K ($T > T_D$) and at 130 K, 100 K, 50 K ($T < T_D$) are shown in Fig. 1. (a). These profiles are measured by cryo-cooler with circulating ^4He gas. Profiles of the Θ-2Θ scans of the (400) reflection at 200 K ($T > T_D$) and at 120 K, 100 K, 50 K ($T < T_D$) are shown in Fig. 1. (b). These profiles are measured by ^3He-^4He dilution refrigerator. From these results we have observed that below T_D the (400) peak splits into two peaks (400) and (040) spectrums when the temperature is lower than the structural phase transition temperature. These profiles contain $Cu_{\alpha 2}$ and the smaller peak, existing in the right shoulder of the peak, is due to the reflection of the K_β line. We have reported the temperature dependence of the (220) peak *d* value for SmFeAsO in ref [5]. The temperature dependence of the d value for this sample shows that the structural phase transition was about 144 K [5].

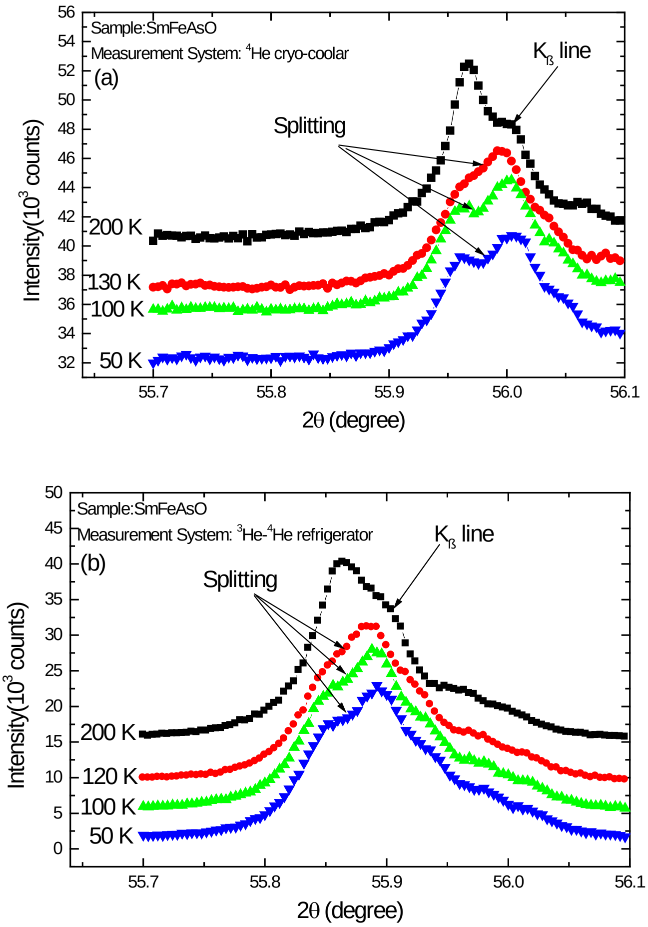

Fig. 1. (a) Profiles of the Θ-2Θ scans of the (400) reflection of the SmFeAsO above and below the transition temperature measured by ^{4}He cryo-cooler. (b) Profiles of the Θ -2Θ scans of the (400) reflection of the SmFeAsO above and below the transition temperature measured by ^{3}He-^{4}He dilution refrigerator.

2.2. *$SmFe_{0.99}Co_{0.01}AsO$* (*x* = 0.01)

Profiles of the Θ -2Θ scans of the (400) reflection of the tetragonal unit cell of $SmFe_{0.99}Co_{0.01}AsO$ at 200 K ($T > T_D$) and at 100 K and 50 K ($T < T_D$) are shown in Fig. 2. (a). These profiles are measured by cryo-cooler with circulating ^{4}He gas. Profiles of the Θ-2Θ scans of the (400) reflection at 200 K ($T > T_D$) and at 100 K and 50 K ($T < T_D$) are shown in Fig. 2 (b). These profiles are measured by ^{3}He-^{4}He dilution refrigerator. From these profiles we have observed that the crystal distortion occurs below the transition temperature. The temperature dependence of the *d* value for this sample will be published in the near future. Our experimental results show that the crystal distortion from the tetragonal to orthorhombic occurs at 134 K.

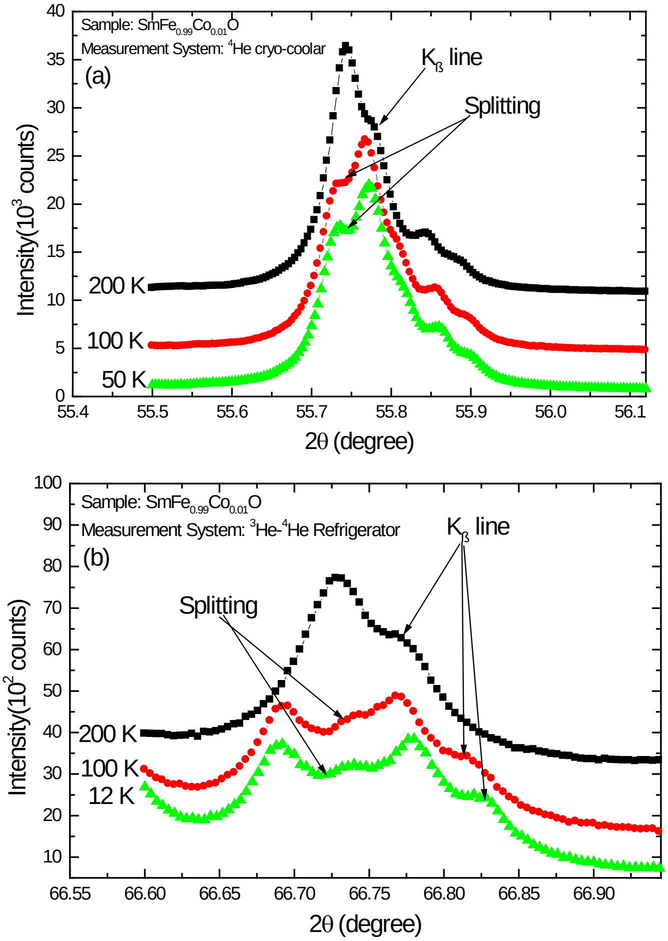

Fig. 2. (a) Profiles of the Θ-2Θ scans of the (400) reflection of the $SmFe_{0.99}Co_{0.01}AsO$ above and below the transition temperature measured by ^4He cryo-cooler. (b) Profiles of the Θ-2Θ scans of the (400) reflection of the $SmFe_{0.99}Co_{0.01}AsO$ above and below the transition temperature measured by ^3He-^4He dilution refrigerator.

2.3. *$SmFe_{0.975}Co_{0.025}AsO$* (*x* = 0.025*)*

Similarly the Profiles of the Θ-2Θ scans of the (400) reflection of the tetragonal unit cell of $SmFe_{0.99}Co_{0.01}AsO$ at 150 K ($T > T_D$) and at 50 K and 12 K ($T < T_D$) are shown in Fig. 3. (a). Profile of the Θ-2Θ scans of the (400) reflection at 150 K ($T > T_D$) and at 50 K and 12 K ($T < T_D$) are shown in Fig. 3 (b). From these profiles we have observed that the crystal distortion occurs below the transition temperature. Our experimental results show that the crystal distortion from the tetragonal to orthorhombic occurs at 118 K.

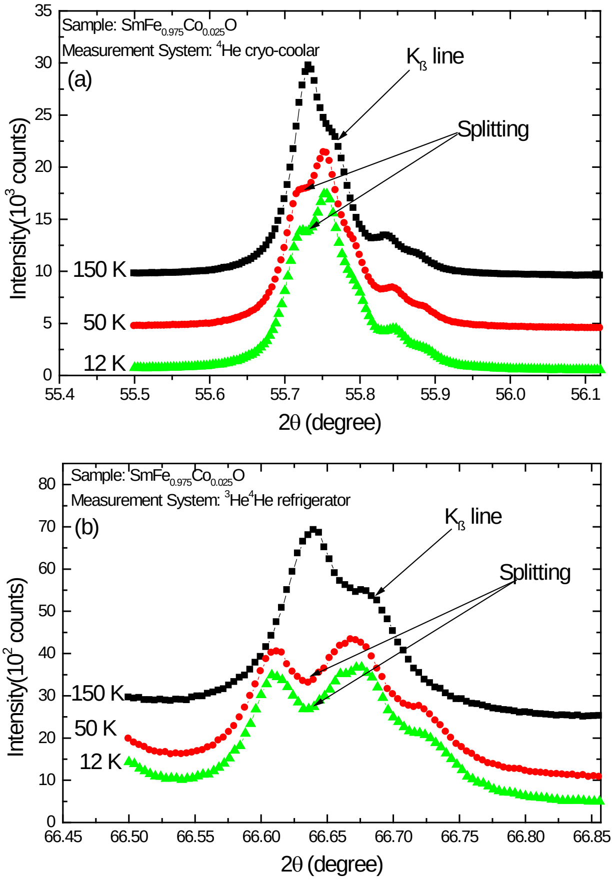

Fig. 3. (a) Profiles of the Θ-2Θ scans of the (400) reflection of the for $SmFe_{0.975}Co_{0.025}AsO$ above and below the transition temperature measured by ^{4}He cryo-cooler. (b) Profiles of the Θ-2Θ scans of the (400) reflection of the for $SmFe_{0.975}Co_{0.025}AsO$ above and below the transition temperature measured by ^{3}He-^{4}He dilution refrigerator.

2.4. $SmFe_{0.925}Co_{0.075}AsO$ (x = 0.075*)*

We did not observe any splitting of the peaks for this sample. But we observed the broadening of peaks below the transition temperature. However Rietveld analysis, which was performed at 7 K and 4 K, suggested the occurrence of the crystal distortion at 4 K [17].

3. Results and Discussions

The structural characterization of $SmFe_{1-x}Co_xAsO$ samples has been reported earlier [18]. They have reported that the Co doping causes the shrinkage of the c-axis significantly, while the a-axis remains nearly unchanged. The unchanged a-axis suggests no significant oxygen deficiency present in our samples. The superconductivity is also observed in the oxygen-deficient $ReFeAsO_{1-x}$, oxygen-deficient in Sr-doped LaFeAsO [14, 21], the F^- doping at the oxygen site in $Re[O_{1-x}F_x]FeAs$ (Re = La and Sm) and also F^- doped in $Ce[O_{1-x}F_x]FeAs$. The entire group of the reported superconductors showed remarkable changes in both *a*-axis and *c*-axis [1, 8, 9]. Since a-axis remains unchanged, so in Co doped compounds superconductivity occurs due to the density of state in the FeAs layers which are increased by the Co doping. Shrinking of the c-axis is observed up to $x = 0.3$ [18, 20]. The shrinkage of *c*-axis occurs because the Co^{2+} ions radius is smaller as compared with Fe^{2+}. This suggests the strengthening of interlayer Coulomb attraction, implying the increase in density of negative charge in FeAs layers by Co doping.

The antiferromagnetic ordering in the parent compound originated from the nearest-neighboring interactions, bridged by As 4*p* orbitals [22-24]. These interactions are antiferromagnetic, which makes a frustrated magnetic ground state. Doping Co into the Fe site, interaction between Co and Fe atoms distort the AFM order. The superconductivity occurs in $SmFe_{1-x}Co_xAsO$ at $x = 0.05$[17-18] suggesting that the Co doping at Fe site plays an important rule due to suppressed structural phase transition and the spin density wave. We are interested to know how the structural phase transition temperature is related to the c-axis. For this purpose we plotted the transition temperature against the lattice constant of the c axis. The values of the *c*- axis with different Co concentrations were taken from ref. [18]. From our experimental result, we observed that T_D for $SmFe_{0.99}Co_{0.01}AsO$, $SmFe_{0.975}Co_{0.025}AsO$ and $SmFe_{0.925}Co_{0.075}AsO$ are 134 K, 118 K and 4 K respectively. Fig. 4 (a) shows the structural phase transition temperature *vs. c*-axis curve. This figure clearly shows that the structural transition temperature is strongly related to the c-axis lattice constant.

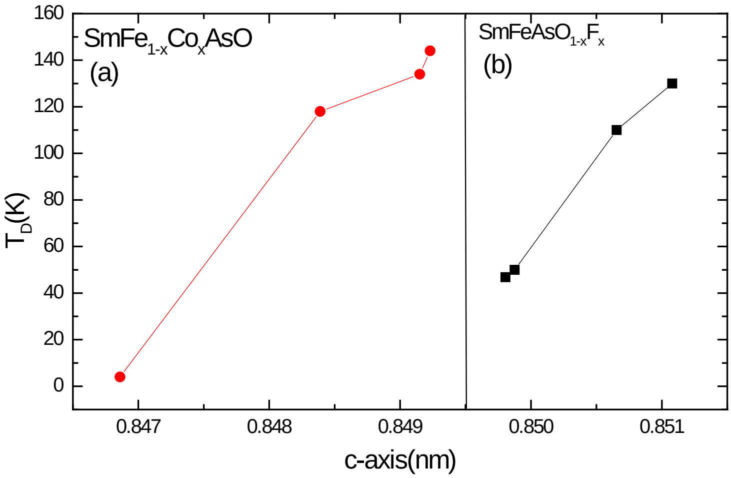

Fig. 4. Structural phase transition *vs. c*-axis curve.

Finally we plot a curve for comparing our experimental results with F^- doped Sm[$O_{1-x}F_x$]FeAs family as shown in Fig. 4 (b). Data are collected from Margadonnal *et al.* [10]. They have studied crystal structure phase transitions of Sm[$O_{1-x}F_x$]FeAs with x = 0, 0.05, 0.10, 0.12, 0.15 and 0.20. The structural phase transition is observed up to x = 0.12 and T_D is approximately 50 K. On the other hand our experimental studies on $SmFe_{1-x}Co_xAsO$ are with x = 0, 0.01, 0.25 and 0.075. The lowest temperature of the structural phase transition was about 4 K with x = 0.075. Experimental findings are listed in Table. 1.

Table. 1.

System	Sm[$O_{1-x}F_x$]FeAs	$SmFe_{1-x}Co_xAsO$
Structural phase transition region	$0 \leq x \leq 0.12$	$0 \leq x \leq 0.075$
Lowest T_D	Approximately 50K	4 K
Shrinking c-axis region	$x \leq 0.20$	$x \leq 0.30$

The Co doped $SmFe_{1-x}Co_xAsO$ system shows both similarity and differences in comparison with the F^- doped Sm[$O_{1-x}F_x$]FeAs system. The similarities are: (1) The structural phase transition in both systems decreases with increasing concentration. (2) The phase diagrams shown in Fig. 4 look very similar. The differences between the two systems are listed in Table 1. Here we noted the following points: (1) The Co doping destroys the AFM, SDW order more strongly. (2) The T_D is significantly lowered in the Co-doped system. (3) In the Co doped system the chemical phase boundary region is longer.

The first and the second can be understood in terms of the variation in exchange interactions. Upon doping Co into the Fe site, the original AFM superexchange interactions may be changed into a double exchange between Co and the Fe atom, which destroys the AFM order. Different number of 3*d* electrons at Fe^{2+} and Co^{2+} validates the double exchange in the form of $Fe^{2+}3d \leftrightarrow As^{3-}4p \leftrightarrow Co^{2+}3d$, analogous to the classical double exchange interaction in perovskite-type manganites [25]. Due to the double coupling in the Co doped system, the structural phase transition driven to the lower temperature with x = 0.075, is much smaller than the F^- doped system. Although at room temperature c-axis shrinkage up to x = 0.30 is observed in the Co doped system, but T_D of this compound is sharply driven to 4 K with x = 0.075. On the other hand at x = 0.03, superconductivity does not appear in this compound [20], due to the disorder effect in (Fe/Co) As layers. In the F^- doped Sm[$O_{1-x}F_x$]FeAs, c-axis shrinkage is observed up to x = 0.02 and the maximum superconductivity occurs at 0.02 concentration [7].

4. Conclusion

From our experimental result we have observed that the transition temperatures T_D for SmFeAsO, $SmFe_{0.99}Co_{0.01}AsO$, $SmFe_{0.975}Co_{0.025}AsO$ and $SmFe_{0.925}Co_{0.075}AsO$ are 144 K, 134 K, 118 K and 4 K respectively. Our experimental results clearly show that as the Co concentration increases, the structural phase transition temperature decreases similar to the shrinkage of the c axis lattice constant. That is, structural transition temperature is strongly related to the c-axis lattice constant. In comparison to its F^- doped $Sm[O_{1-x}F_x]FeAs$ system the phase diagram shows the similarity, but in the Co-doped system the structural phase transition is driven to more lower temperatures with small concentration as compared to F^- doped $Sm[O_{1-x}F_x]FeAs$ system.

We have observed that the structural phase transition temperature decreases with shrinking lattice constant of c-axis similar to the decreasing of the structural phase transition temperature with increasing Co concentration.

References

1. Y. Kamihara, T. Watanabe, M. Hirano, and H. Hosono, J. Am. Chem. Soc. **130**, 3295 (2008). http://dx.doi.org/10.1021/ja800073m
2. J. Dong, H. J. Zhang, G. Xu, Z. Li, G. Li, W. Z. Hu, D. Wu, G. F. Chen, X. Dai, J. L. Luo, Z. Fang, and N. L.Wang, EPL **83**, 27006 (2008). http://dx.doi.org/10.1209/0295-5075/83/27006
2. C. de la Cruz, Q. Huang, J. W. Lynn, Jiying Li, W. Ratcliff II, J. L. Zarestky, H. A. Mook, G. F. Chen, J. L. Luo, N. L. Wang, and P. Dai, Nature **453**, 899 (2008). http://dx.doi.org/10.1038/nature07057
4. Q. Huang, J. Zhao, J. W. Lynn, G. F. Chen, J. L. Luo, N. L.Wang, and P. Dai, Phys. Rev. B **78**, 054529 (2008). http://dx.doi.org/10.1103/PhysRevB.78.054529
5. Y. Luo, Q. Tao, Y. Li, X. Lin, L. Li, G. Cao, Z. Xu, Y. Xue, H. Kaneko, A.V. Savinkov, H. Suzuki, C. Fang, and J. Hu, Phys. Rev. B **80**, 224511 (2009). http://dx.doi.org/10.1103/PhysRevB.80.224511
6. H. Takahashi, K. Igawa, K.Arii, Y. Kamihara, M. Hirano, and H. Hosono. Nature **453**, 376 (2008). http://dx.doi.org/10.1038/nature06972
7. R. H. Liu, G. Wu, T. Wu, D. F. Fang, H. Chen, S. Y. Li, K. Liu, Y. L. Xie, X. F. Wang, R. L. Yang, L. Ding, C. He, D. L. Feng, and X. H. Chen, arXiv:0804.2105v3 (2008).
8. G. F. Chen, Z. Li, D. Wu, G. Li, W. Z. Hu, J. Dong, J. L. Luo, and N. L. Wang, Phys. Rev. Lett. **100**, 247002 (2008). http://dx.doi.org/10.1103/PhysRevLett.100.247002
9. X. H. Chen, T. Wu, R. H. Liu, H. Chen, and D. F. Fang, Nature **453**, 761 (2008). http://dx.doi.org/10.1038/nature07045
10. S. Margadonnal. Y. Takabayshi, M. T. McDonald, M. Brunelli, G. Wu, R.H. Liu, X.H. Chen, and K. Prassides, Crystal structure and phase transitions across the metal-superconductor boundary in the $SmFeAsO_{1-x}F_x$ ($0\leq x \leq 0.20$) family, arXiv: 0806.3962 (2008).
11. G. F. Chen, L. Zheng, W. Dan, D. Jing, L. Gang, H. W. Zheng, Z. Ping, L. J. Lin, and W. N. Lin. Chin. Phys. Lett. **25**, 2235 (2008).
12. P. Cheng, L. Fang, H. Yang, X. Zhu, G. Mu, H. Luo, Z. Wang, and H. H. Wen, Science in China G51, 719 (2008).
13. C. Wang, L. Li, S. Chi, Z. Ren, Y. Li, Y. Wang, X. Lin, Y. Luo, S. Jiang, X. Xu, G. Cao, and Z. Xu, EPL **83**, 67006 (2008). http://dx.doi.org/10.1209/0295-5075/83/67006
14. Z. A. Ren, G. C. Che, X. L. Dong, J. Yang, W. Yi, X. L. Shen, Z. C. Li, L. L. Sun, F. Zhou, and Z. X. Zhao, EPL **83**, 17002 (2008). http://dx.doi.org/10.1209/0295-5075/83/17002
15. V. P. S. Awana, A. Vajpayee, and H. Kishan, J. Phys.: Cond. Matt. Fast Track Commun. **20**, 292201 (2008).
16. G. Xu, W. Ming, Y. Yao, X. Dai, S.C. Zhang, and Z. Fang, Europhys. Lett. **82**. 67002 (2008). http://dx.doi.org/10.1209/0295-5075/82/67002
17. H. Kaneko, Y. Yun, S. Naher, A. Savinkov, H. Suzuki, Y. K. Li, Q. Tao, G. H. Cao, and Z. A. Xu (to be published LT26 in Journal of Low Temperature Physics).
18. C. Wang, Y. K. Li, Z. W. Zhu, X. Lin, Y. K. Luo, S. Chi, L. J. Li, Z. Ren, M. He, H. Chen, Y. T. Wang, Q. Tao, G. H. Cao, and Z. A. Xu, Phys. Rev. **B 79**, 054521 (2009). http://dx.doi.org/10.1103/PhysRevB.79.054521

19. V. P. S. Awana, A. Vajpayee, A. Pal, M. Mudgel, R. S. Meena, and H. Kishan, J. Supercond. Novel Magn. **22**, L623-L626 (2009). http://dx.doi.org/10.1007/s10948-009-0498-1
20. V. P. S. Awana, A. Vajpayee, A. Pal, M. Mudgel, R. S. Meena, and H. Kishan, J. Appl. Phys. **107**. O9E 146 (2010). http://dx.doi.org/10.1063/1.3366601
21. H. H. Wen, G. Mu, L. Fang, H. Yang, and X. Zhu, EPL **82**, 17009 (2008). http://dx.doi.org/10.1209/0295-5075/82/17009
22. T. Yildirim, Phys. Rev. Lett. **101**, 057010 (2008). http://dx.doi.org/10.1103/PhysRevLett.101.057010
23. Q. Si and E. Abrahams, Phys. Rev. Lett. **101**, 076401 (2008). http://dx.doi.org/10.1103/PhysRevLett.101.076401
24. F. Ma, Z. Y. Lu, and T. Xiang, Phys. Rev. B **78**, 224517 (2008). http://dx.doi.org/10.1103/PhysRevB.78.224517